Polarforschung 73 (2/3), 49 – 57, 2003 (erschienen 2006)

Metabasite Basement of the Voikar Island Arc in the Polar Urals

by Dmitry N. Remizov[1]

Abstract: High-pressure/low-temperature metabasites occupy a definite geological position within the structure of the Polar Urals and have a very important bearing on the understanding of the early history of the Ural Mountains. Recently obtained geological, petrographic, geochemical and isotope data allow some conclusions on this history. The metabasites of the Khord"yus and Dzela complexes contain relics of a Neoproterozoic (578 ±8 Ma) oceanic crust. This crust formed part of the base of the early Paleozoic (500 Ma) ensimatic island arc and experienced Ca-Al-Si±Na metasomatism and, probably, partial melting with the formation of boninite melts. However, so far no boninite volcanics have been found. The metabasites at the base of the island arc took part in the collision and as a consequence experienced glaucophane schist and greenschist facies metamorphism during the collision and obduction over the passive Baltic margin 350 ±11 Ma ago.

Zusammenfassung: Hochdruck-Niedrigtemperatur-Metabasite nehmen in der Struktur des Polaren Urals eine bestimmende geologische Position ein und besitzen eine wichtige Bedeutung für das Verständnis der frühen Entstehungsgeschichte des Urals. Neue geologische, petrographische, geochemische und Isotopiedaten gestatten einige Schlussfolgerungen zu dieser Geschichte. An den Metabasiten der Khord"yus- und Dzela-Komplexe sind Reste einer neoproterozoischen (578 ±8 Ma) ozeanischen Kruste beteiligt. Diese Kruste wurde in die Basis des frühpaläozoischen (500 Ma) ensimatischen Inselbogens einbezogen, erfuhr eine spezifische Ca-Al-Si±Na-Metasomatose und möglicherweise eine partielle Aufschmelzung mit Bildung boninitischer Schmelzen. Bisher konnten jedoch keine Boninite gefunden werden. Als Bestandteil der Basis des Inselbogens erfuhren die Metabasite eine Glaukophanschiefer- und Grünschiefer-Metamorphose während der Kollision und Obduktion über den passiven Kontinentalrand von Baltica vor 350 ±11 Ma.

INTRODUCTION

The present contribution is based on the book "The Paleozoic Island Arc System of the Polar Urals" by REMIZOV (2004, in Russian). The book deals with the results of studies carried out up to 2001 with respect to the geological structure of the Polar Urals. More recent field work carried out during the Polar Urals Expedition project (PURE) in 2001-2003 by the German Federal Institute for Geosciences and Natural Resources (BGR) in Hannover, the Institute of Geology of the Russian Academy of Science in Syktyvkar and the Geological Institute of the Russian Academy of Science in Moscow has not been covered in this paper, but will be published in due course. Thus, the present paper reflects exclusively the views of the author prior to the beginning of the PURE project.

GEOLOGY

The Polar Urals are the northernmost part of the Ural Mountains and are located between 65-68 °N. The formations of the Voikar island arc crop out in the southern part of the Polar Urals (Fig. 1). The main structures of the Urals trend NE-SW, parallel to the Main Uralian thrust fault (MUF). The MUF is a collision suture which separates the formations of the east European continental margin in the northwest from high-grade metamorphic rocks of the allochthonous Khord"yus and Dzela blocks and the ophiolites of the Voikar ultramafics in the southeast. The formations of the East European continental margin are characterized by rock sequences of two extensive facies zones, the Elets shelf zone and the Lemva deep water zone (PUCHKOV 1979, YUDIN 1994 and other). The sedimentary sequences of these zones were deposited from the Late Cambrian to Early Carboniferous coevally with the existence of the Uralian paleo-ocean. The MUF is made of a "greenschist" melange attaining a width of 15 km.

The hanging wall of the MUF is composed of rocks of the Uralian paleo-ocean crust, which were the subject of our studies. Bordering the MUF melange on the southeast, a strip of high-pressure/low-temperature metamorphic rocks crops out along the almost entire NE-SW extent of the Voikar zone. The most extensive blocks within this strip, which are mainly represented by metamorphic gabbronorite and small bodies of ultramafic metamorphic rocks, are exposed in the Khord"yus and Dzela complexes (Fig. 1).

Further towards the southeast allochthonous blocks of the Voikar ultramafic (ophiolitic) massif occur. The boundary between the high-grade metamorphic rocks and the ophiolites is marked by a thin zone of serpentinite. These ultramafic blocks, which became allochthonous either together with the high-grade metamorphics or separately from them, have been interpreted differently by various workers:
i) as the western prolongation of the Paleozoic Voikar massif (PERFIL'EV 1979, SAVEL'EVA 1987, and others),
ii) as the northern prolongation of the Uralian platiniferous belt (EFIMOV & POTAPOVA 1990, 2000), and
iii) as tectonic blocks of the Paleoproterozoic basement of the Russian platform (PYSTIN 1994).
It is inferred that the high-grade metamorphic rocks are, together with the ultramafic massifs, gabbro, granitoids and volcano-sedimentary formations of the Voikar island arc, a deep-seated part of this arc (REMIZOV 2000).

Southeastwards from the Voikar ultramafics is a strip of variable width consisting of rocks of a dunite-wehrlite-clinopyroxenite complex. It occurs between the Voikar ultramafics and the "eastern" gabbro. Further towards southeast the gabbro is replaced by amphibolites with migmatite bodies of plagiogranite (Sob' Complex, REMIZOV 2004), tonalite-trondhjemite massifs of the intrusive Kongor Complex (REMIZOV 2004), which is overlain by andesites. All these complexes from amphibolite to andesite are characterized by a gradual transition and are interpreted as formations belonging to the late Silurian to Middle Devonian intra-oceanic island arc. Gabbrono-

[1] Institute of Geology, Komi Science Center, Russian Academy of Science, 54 Pervomayskaya Street, 167610 Syktyvkar, Russia, <kirul@rol.ru>

Manucript received 26 October 2004, accepted 22 November 2005

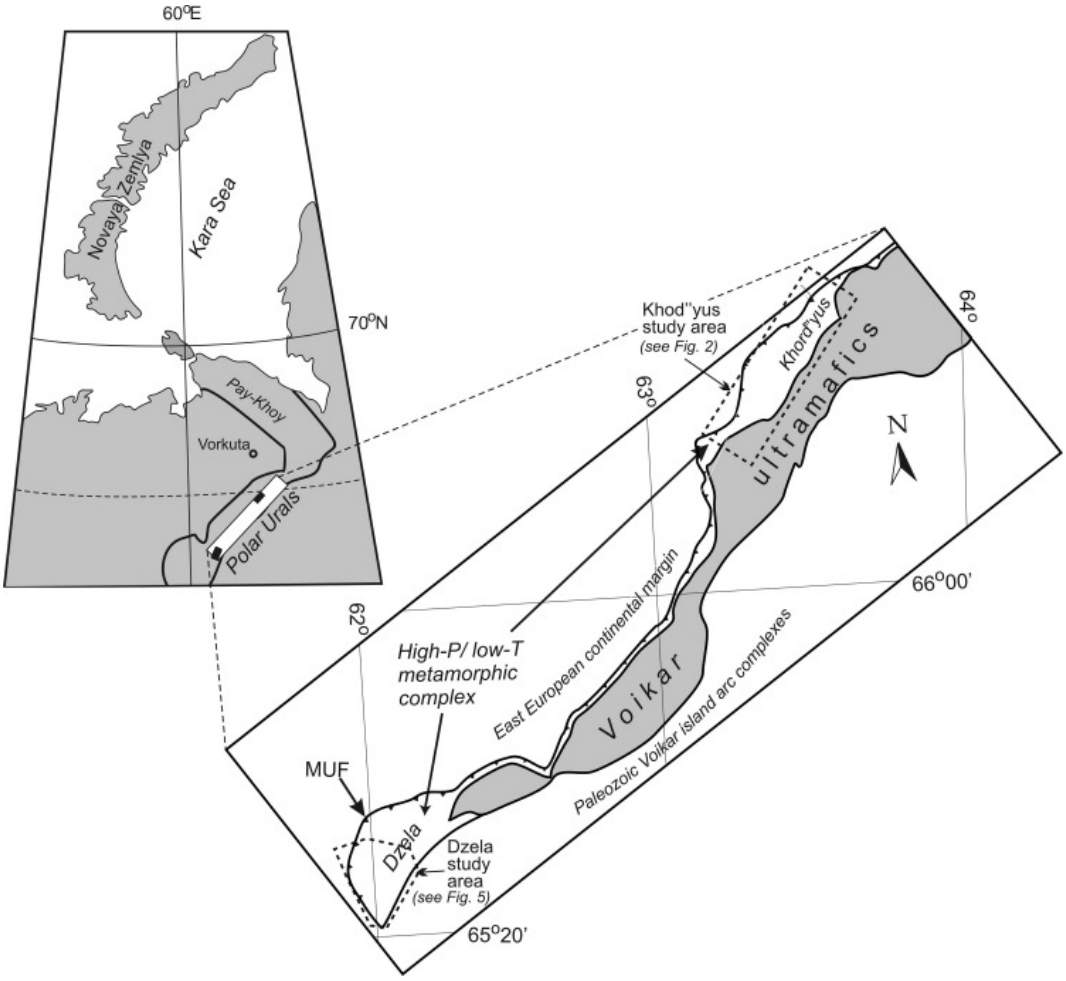

Fig. 1: The location of the metamorphic complexes of the Voikar massif. (MUF = Main Uralian thrust fault).

Abb. 1: Lage der metamorphen Komplexe des Voikar-Massivs.

rites (to quartz diorite) and alaskite of the Yanaslor Complex (REMIZOV 2004) intrude the formations mentioned above and are associated with Late Devonian to early Carboniferous dacites and rhyolites. Formerly, these formations were interpreted as formations belonging to an active margin of the Cordil-lera type (YAZEVA & BOCHKAREV 1984) or as an ensialic island arc (REMIZOV 2000). The formations of the late Silurian to Middle Devonian intra-oceanic island arc are separated from the Late Devonian to early Carboniferous ensialic island arc formations by a major fault zone, which is associated with volcano-sedimentary molasse of late Eifelian to early Givet-ian age. The molasse was deposited prior to the collision of the island arc with the passive continental margin in late Carboniferous to Permian time.

VOIKAR METAMORPHIC COMPLEXES

The Voikar metamorphic complexes occur between the MUF and the Voikar ultramafic massif and comprise, from northeast to southwest, the Khord"yus and Dzela blocks (Fig.1).

Khord"yus metamorphic complex

The geological structure and composition of the Khord"yus metamorphic complex have been described by DOBRETSOV (1974), PERFIL'EV (1979), SAVEL'EVA (1987), VALIZER & LENNYKH (1988), EFIMOV & POTAPOVA (1990, 2000), KOSTYUKHIN & REMIZOV (1995) and others. SAVEL'EVA (1987) grouped this part to the Khulga nappe with the Voikar ultramafics. PERFIL'EV (1979) considered the Khord"yus block as the base of a huge fold of oceanic lithosphere with an ultramafic core. This view is also taken by the German counterparts of the PURE project F. Schäfer and K.-P. Burgath (pers. comm.).

EFIMOV & POTAPOVA (1990, 2000) distinguished three metabasite complexes within the Khord"yus structure (Fig. 2): i) the Pal'nikshor metavolcanic series of basalts and rhyolites, ii) the Khord"yus granulite-amphibolite complex including high-Sr gabbro and gabbronorite, and iii) the Levolagorta complex composed of olivine-bearing anorthosite gabbro partly metamorphosed under granulite-facies conditions. The Levolagorta complex is considered to be part of an ophiolite and to correspond to the "eastern" gabbro. KOSTYUKHIN & REMIZOV (1995) also concluded that the Khord"yus complex is heterogeneous and inferred an oceanic origin for the western high-Sr amphibolites.

The Khord"yus metamorphic complex, which has glaucophane schists at the base, represents a tectonic nappe that was thrust over sedimentary rocks of the Lemva allochthon (DOBRETSOV 1974, SAVEL'EVA 1987). The upper part of the glaucophane schists consists of garnet amphibolite, zoisite-garnet amphibolite, and zoisite amphibolite with bodies of plagiogranite gneiss and dykes of plagiogranite. Huge concordant bodies of gabbronorite and blastomylonite up to 2.5 km thick overlie this association at the most extensive

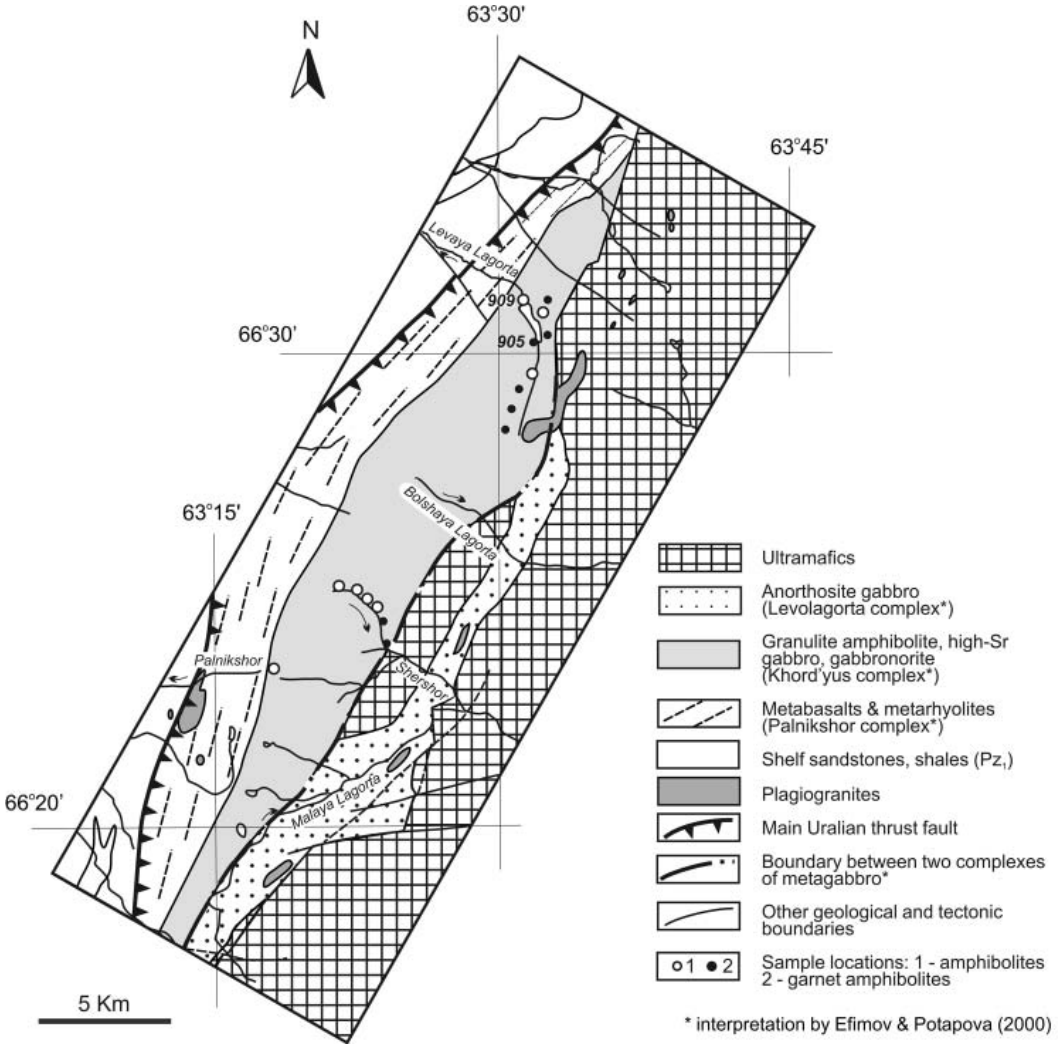

Fig. 2: Geological map of the Khord"yus metamorphic complex (for location see Fig. 1).

Abb. 2: Geologische Karte des metamorphen Khord"yus Komplexes (Lage in Abb. 1).

occurrence of the nappe (as in the Dzela Complex). They show a transition into zoisite and garnet amphibolite containing rafts and lenses of amphibolitised ultramafic rocks. The metamorphic structures of the blastomylonites, which were derived from gabbronorite, are distinctly discordant to the NE-SW trending structures of the amphibolites (SAVEL'EVA 1987).

Petrology

Estimates of the conditions of formation of the Khord"yus amphibolites based on garnet-amphibole equilibrium give values of P_{total} = 8.1 kb and T = 660 °C (KOSTYUKHIN & REMIZIOV 1995). The Fe/(Fe+Mg) *versus* Fem/(Fem+An) diagram (Fig. 3) shows a slightly lower iron content of the garnet-free amphibolites in comparison with the garnet-bearing amphibolites. The area of the gabbro protolith is characterized by the high-pressure field (over 15 kb). Some points in the diagram are located in the low-pressure area what reflects the evolution trend of the gabbro melt at low pressure. The decrease in the iron content of the femic minerals (Fe/[Fe+Mg]) and in the femic rock index (Fem/[Fem+ An]) during the evolution is a hint to the calc-alkaline differentiation trend of the protolith melt. In the AF'M diagram the amphibolites show a calc-alkaline trend, which is, however, somewhat tholeiitic (Fig. 4).

The Khord"yus garnet-zoisite amphibolites are characterized by a higher content of Ti, Na, K, Sr and a lower content of Fe, Mg, Ca, Cr than the garnet-free amphibolites (EFIMOV & POTAPOVA 1990; see also Tab. 1). The geochemical data suggest that the Khord"yus gabbro protolith was heterogeneous in composition. The geochemical data of Khord"yus rocks are sparse (Tab.1) and will be discussed below together with the data from the Dzela Complex.

Dzela metamorphic complex

The general structure of the Dzela Complex (Fig. 5) is a fold trending parallel to the MUF. In the southern part of the central zone, pegmatites containing giant hornblendes (5-15 cm) occur within garnet-bearing amphibolites. The ultramafic Dzela massif is situated in the eastern part of the complex. The central part of the massif is composed of garnet-bearing pyroxenites, dunites and lherzolites surrounded by melanocratic garnet-amphibolites. A serpentinite melange cuts the SE part of the Dzela massif. The melange contains small fragments of Lower Ordovician lilac-coloured schist, which have a wide distribution in the west along the passive margin of the Urals. Probably, they are of late-collision or later origin. North of the massif, homogeneous mesocratic to leucocratic deformed norites and gabbronorites occur, the composition of which changes to quartz diorite. Towards the west amphibolite and

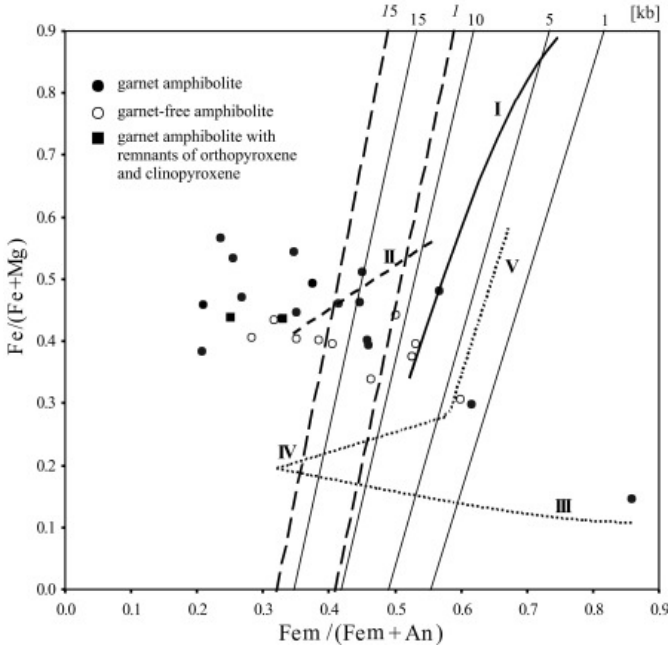

Fig. 3: Amphibolites of the Khord"yus metamorphic complex in the Fe/(Fe+Mg) *vs.* Fem/(Fem+An) diagram of FERSHTATER (1987). Fem = Di+Hy+Ol (from CIPW norm). Figures on the upper margin of the diagram: the pressure [kb] of the corresponding eutectic. Dashed lines = An-Opx eutectic at 15 kb and 1 kb, thin continuous lines = An-Cpx-Opx eutectic at 15 kb, 10 kb and 1 kb; I = settlement trend of Skaergaard; II = gabbro of Platinum Belt of Urals; III to V = Kempirsay-Chabarny ophiolitic complex, III = layered series, IV = Di-gabbro, V = basalts.

Abb. 3: Amphibolite des metamorphen Khord"yus-Komplexes im Diagramm Fe/(Fe+Mg) gegen Fem/(Fem+An) nach FERSHTATER (1987).

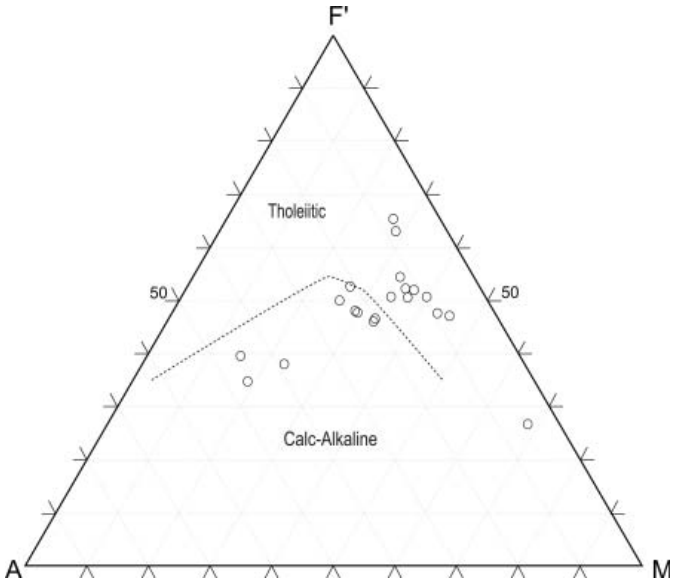

Fig. 4: AF'M diagram (after IRVINE & BARAGAR 1971) for amphibolites of the Khord"yus metamorphic complex.

Abb. 4: AF'M-Diagramm (nach IRVINE & BARAGAR 1971) für Amphibolite des metamorphen Khord"yus-Komplexes.

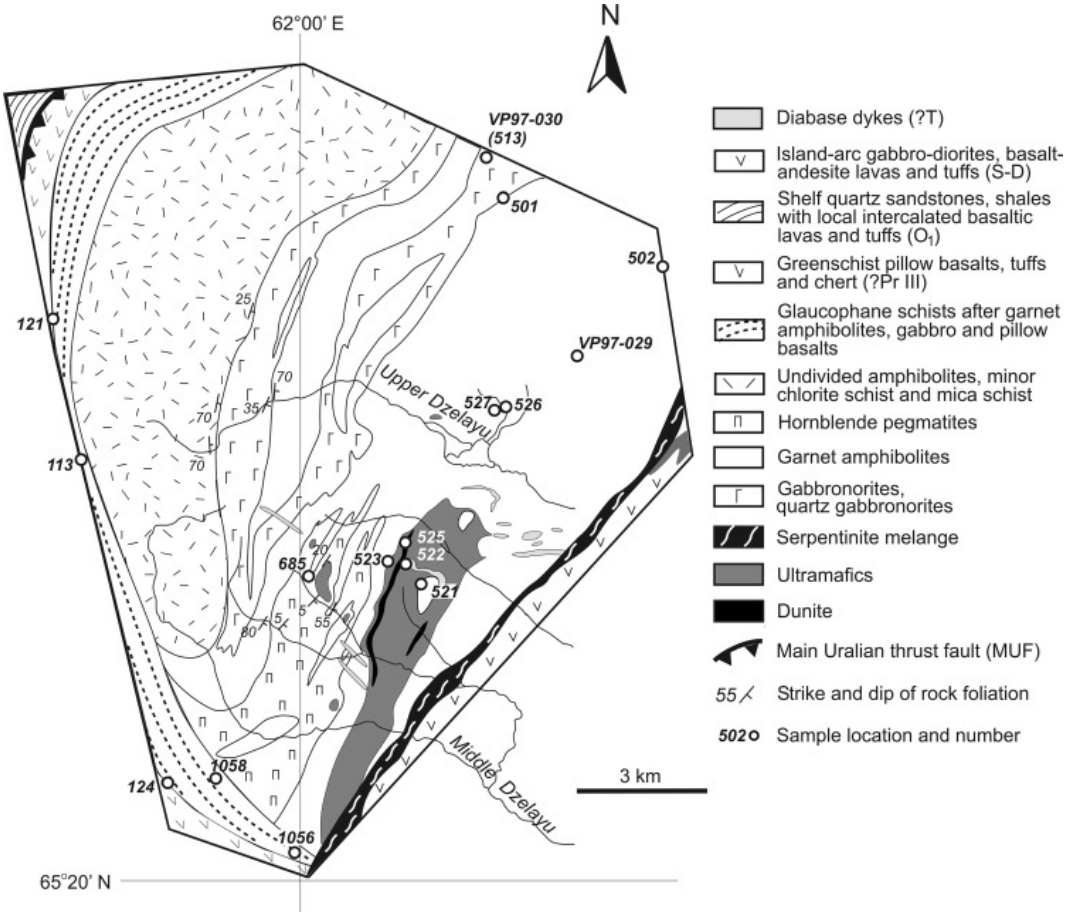

Fig. 5: Geological map of the Dzela metamorphic complex (for location see Fig. 1).

Abb. 5: Geologische Karte des metamorphen Dzela-Komplexes (Lage in Abb.1).

gabbronorite are bordered by chlorite schists and mica schists at the contact with amphibolite. Further west the Dzela block is bordered by a strip of glaucophane schist. In the westernmost part the outermost member of the stratigraphic succession of the Dzela Complex consists of greenschist facies rocks of meta-pillow basalts, metabasalts with relics of ophitic structure, metasedimentary rocks, and jasper. The greenschists are in contact with Lower Ordovician deposits of the East European passive margin along the tectonic boundary of MUF.

Metamorphic rocks and processes

During amphibolite facies metamorphism the pyroxenites and gabbros were transformed into garnet hornblendite or garnet-plagioclase amphibolite, respectively. The garnet amphibolites contain ≥10-30 % garnet as the main rock-forming mineral. Plagioclase and hornblende have been extensively altered by metasomatic "zoisitisation" at all structural levels. Metasomatic fluids added Al, Ca and a small amount of Na. The final stage in this process is the formation of bimineralic zoisite-kyanite rocks. The zone of garnet-glaucophane and glaucophane schists can be traced around the western periphery of the gabbronorite and amphibolite (Fig. 5). In the west the entire structure is bordered by epidote-chlorite-albite-quartz schists with an admixture of calcite. These green-coloured and grey-green rocks, which can be readily mapped in the field, are intensely folded. In thin-section nematogranoblastic structure with relics of ophitic texture suggests a basalt or basaltic pyroclastic rock protolith. In addition, schists containing relics of glaucophane occur, as well as metasedimentary rocks containing abundant calcite and quartz. Altered basalts and jasper are also present. Locally, the greenschist metamorphism is seen to be superimposed on the glaucophane-forming processes. This is concluded from the petrographic studies, e.g., by the occurrence of relics of glaucophane and garnet in greenschists and from the geochemical results, particularly the variation of the Sr content and the REE pattern of different glaucophane-schist types (GL-1 and GL-2, Tab. 1). Thus, it can be inferred that an upper layer of the oceanic crust exists here, hence the rock association metabasalt and jasper and their characteristic chemical composition.

Geochemistry

High-field-strength elements (HFSEs) and rare earth elements (REEs) are the most stable elements during metamorphic processes (e.g., see POLAT et al. 2003 for amphibolite facies, MOCEK 2001 for glaucophane schist facies, BECKER et al. 2000 for eclogite facies). Consequently, the abundances of HFSE and REE are most likely to preserve the primary relationships. The data given in Table 1 were obtained by neutron activation in the Institute for Geochemistry of the Russian Academy of Science (Moscow), using the chondrite normalized element concentration of BOYNTON (1984).

Ultramafic rocks

Harzburgite (sample 522/2), lherzolite (502/2) and dunite (525/1) have high contents of MgO (28-44 wt.% of the water-free rock material), and low contents of Al_2O_3 (1.53-7.99 wt.%), CaO (0.94-4.99 wt.%) and TiO_2 (0.03-0.24 wt.%). They show a relative depletion of Sc (5-13 ppm) and correspondingly high contents of Cr, Ni, and Co (up to almost 16000, 1400, 170 ppm, respectively). Ultramafic rocks of the Dzela Complex have low contents of REE (Fig. 6), typical for ultramafic rocks of depleted mantle and undifferentiated island arcs, but they cannot be attributed to either with any reliability owing to the paucity of geochemical data. However, all samples show a clear negative Eu anomaly, providing a hint that they might have been residual after a basaltic melt fraction had separated off. Only the garnet-bearing pyroxenite (685/1) shows a positive Eu anomaly (Eu/Eu* = 2.36).

Plagioclase lherzolite (502/2) has a special position and can be classified as an ultramafitite enriched in plagioclase. Most likely, these rocks were primary dunites that experienced Ca-Al-Si ±Na metasomatism. The secondary formation of plagioclase is documented by field and microscopic observations. Addition of Ca was not accompanied by enrichment in Eu; however, the LREE (La, Ce, Pr) did increase. This sample and the garnet pyroxenite (685/1) show a relative enrichment of the light and heavy REE in relation to the medium REE. The pattern of REE distribution is very similar to that shown by boninites.

Gabbroic rocks

The fresh gabbronorites have 40-51 wt.% SiO_2 and high Al_2O_3 (>18 wt.%), CaO (>15 wt.%), low to moderate MgO (3-9 wt.%), and low TiO_2 (<0.8 wt.%). The metamorphic transformation of gabbro to garnet amphibolite has been observed in the field. Consequently, chondrite-normalized REE compositions of gabbro and its inferred metamorphic equivalents are plotted together (Fig. 6). The Dzela quartz gabbronorite (513) has enriched chondrite-normalized light REE relative to heavy REE ($[La/Lu]_N$ = 2.74), with absolute concentrations between chondrite and NMORB. Garnet amphibolite has a variable chondrite-normalized REE pattern, but generally defines a weak (526/1) to moderate (523/2) LREE enrichment ($[La/Sm]_N$ = 0.30). The latter is accompanied by a pronounced negative Eu anomaly (Eu/Eu* = 0.31). In other samples, an Eu anomaly is variable, i.e. negative to slightly positive (Eu/Eu* = 0.31-1.20) or absent.

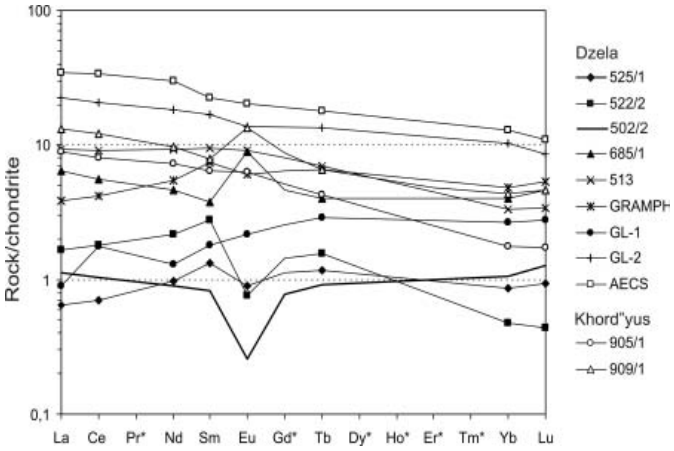

Fig. 6: Chondrite-normalized rare-earth element distributions of the Dzela and Khord"yus metamorphic complexes (for specimen numbers see Tab. 1, and for specimen localities see Fig. 5). GRAMPH, GL-1, GL-2, and AECS are averages (see Tab. 1).

Abb. 6: Chondrit-normierte Seltene-Erden-Verteilungsmuster der metamorphen Dzela- und Khord"yus-Komplexe. (Probennummern in Tab. 1, Lage der Probenpunke in Abb. 4). GRAMPH, GL-1, GL-2 und AECS sind Mittel-werte (siehe Tab. 1).

No.	1	2	3	4	5	6	7	8	9	10	11	12	13
SAMPLE	DR-525/1	DR-522-2	DR-502/2	DR-685/1	DR-521/2	DR-501/1	DR-513	DR-521/3	DR-523/2	DR-526/1	DR-527/1	DR-1056/1	DR-1056/2
ROCK	D	HB	PLLZ	GRPX	PX	GN	QGN	AMPHPX	GRAMP	GRAMP	MIAMP	GL-1	GL-1
SiO_2	33.97	37.34	38.52	39.37	40.89	40.66	51.25	41.73	40.43	48.14	48.92	40.68	38.25
TiO_2	0.03	0.24	0.05	1.863	1.25	0.57	0.79	1.03	0.91	0.99	0.34	0.28	0.20
Al_2O_3	1.53	2.33	7.99	15.93	13.56	19.02	21.87	6.59	13.35	13.60	18.01	17.74	19.28
Fe_2O_3	5.54	6.58	7.06	19.86	5.63	7.03	3.54	8.39	5.10	5.18	4.66	4.10	3.81
FeO	6.82	9.98	6.21	-	8.28	6.57	5.10	10.43	10.33	7.55	3.72	2.62	2.19
MnO	0.15	0.39	0.17	0.414	0.15	0.12	0.18	0.32	0.19	0.26	0.17	0.10	0.08
MgO	43.97	35.97	28.17	7.95	13.36	8.98	3.18	19.03	13.45	9.30	7.76	16.79	12.28
CaO	0.94	2.97	4.99	11.70	12.33	15.08	9.63	10.75	13.44	10.56	11.21	10.66	16.84
Na_2O	0.07	0.15	0.24	1.66	2.09	0.52	3.60	0.59	0.99	1.76	2.05	1.90	1.59
K_2O	0.02	0.02	0.02	0.29	0.45	0.02	0.07	0.02	0.12	0.10	0.17	0.02	0.02
P_2O_5	0.05	0.05	0.05	0.009	0.05	0.05	0.24	0.05	0.05	0.08	0.05	0.05	0.05
LOI	6.62	4.06	6.61	0.59	2.03	1.45	0.58	1.15	1.69	2.48	2.99	5.01	5.46
TOTAL	99.71	100.07	100.07	100.12	100.05	100.07	100.02	100.07	100.05	100.00	100.05	99.95	100.04
La	0.20	0.51	0.35	1.99	-	-	2.89	1.50	0.58	1.81	8.89	0.23	0.33
Ce	0.57	1.46	0.84	4.50	-	-	7.40	4.04	1.80	5.00	19.10	0.75	2.11
Nd	0.58	1.30	0.54	2.76	-	-	5.52	3.80	2.23	4.32	10.80	0.69	0.85
Sm	0.26	0.54	0.16	0.73	-	-	1.85	1.57	1.18	1.69	2.68	0.38	0.32
Eu	0.066	0.056	0.019	0.66	-	-	0.67	0.24	0.13	0.76	0.55	0.176	0.14
Tb	0.055	0.074	0.074	0.19	-	-	0.33	0.33	0.23	0.39	0.53	0.19	0.086
Yb	0.18	0.099	0.22	0.84	-	-	0.70	0.97	0.63	1.40	1.50	0.73	0.37
Lu	0.03	0.014	0.041	0.15	-	-	0.11	0.16	0.10	0.24	0.25	0.12	0.057
TOTAL REE	1.941	4.053	2.213	11.82	-	-	19.47	12.61	6.88	15.61	44.30	3.27	4.263
Rb	24.9	14	14	42.6	-	-	20	20.1	22	29	20.7	0	0
Cs	0	0.48	0	0.7	-	-	0	0.38	1.21	0.47	0	-	-
Sr	0	54	245	550	-	-	1.080	0	195	735	210	681	755
Ba	145	530	250	510	-	-	285	1.890	165	220	166	-	-
Cr	4330	15785	62.3	38.4	-	-	33.2	145.8	56.7	49.6	77.8	45.5	38.2
Co	138.4	172.4	109.4	27.7	-	-	26.1	80.9	53.9	35.6	18.9	46	24.9
As	1.92	10.2	0.83	3.95	-	-	0	6.51	4.24	10.1	4.43	-	-
Sb	0.18	0.34	0.25	0.11	-	-	1.44	0.92	0.14	0.6	0.16	-	-
Sc	4.79	13	5.82	33.80	-	-	22.3	69.2	62.50	54.4	33.6	45.7	36
Hf	0.36	0.46	0.26	0.20	-	-	0.48	0.92	0.45	0.33	5.18	0	0
Th	0.18	0.51	0	0.95	-	-	0.22	0.60	0.21	0.13	3.97	0	0
U	3.59	1.56	0.62	1.47	-	-	1.10	1.66	2.07	1.47	0.93	-	-
Ta	0.095	0	0	0	-	-	0.32	0	0	0	0	0	0
Zr	10	32	455	35	-	-	120	45	47	90	110	-	-
Ni	1430	1190	100	90	-	-	120	160	110	40	0	-	-
Se	1.9	1.5	3.8	1.9	-	-	5.1	3.2	2.0	0.1	3.1	-	-
Zn	90	110	40	0	-	-	80	200	10	310	10	-	-

Tab. 1: Representative bulk-rock chemistry (wt.%) and trace element data (ppm) for rocks from the Dzela (1-22) and Khord"yus (23-26) complexes.
Rock types: D = dunite; HB = harzburgite; PLLZ = lherzolite with metasomatic plagioclase; PX = pyroxenite; GRPX = garnet pyroxenite; GN = gabbronorite; QGN = quartz-bearing gabbronorite; AMPH = amphibolite; AMPHPX = metapyroxenite amphibolite; GRAMP = garnet amphibolite; MIAMP = mica-bearing amphibolite; GL = glaucophane schist; AECS = greenschist metabasalt (albite-epidote-chlorite slate); 0 = values below detection limit.

Tab. 1: Repräsentative Analysen des Hauptelement- (in %) und Spurenelement-Chemismus (in ppm) von Gesteinen der metamorphen Dzela- (Spalten 1-22) und Khord"yus-Komplexe (Spalten 23-26).

The REE pattern in Khord"yus amphibolites is similar to that in the Dzela gabbronorites and amphibolites, but the difference between light and heavy REE is greater ($[La/Lu]_N$ = 27-49). However, the difference may be due to the paucity of samples.

Rocks metamorphosed under glaucophane and greenschist facies

Two compositional groups can be defined on the basis of major-element oxide variations. One group has low SiO_2 (38-41 wt.%), high Al_2O_3 (18-19 wt.%), low to moderate CaO (11-17 wt.%), high MgO (12-17 wt.%), and extremely low TiO_2 (<0.3 wt.%). The other group has higher SiO_2 (48-51 wt.%), with moderate Al_2O_3 (13-16 wt.%), low to moderate CaO (4-11 wt.%), moderate MgO (7-10 wt.%), and low TiO_2 (c. 1 wt.%). These two groups of Dzela blueschist (glaucophane schist) and greenschist (albite+epidote+chlorite metabasalt) also show distinct chondrite-normalized REE patterns (Fig. 6). Samples of blueschist and a greenschist with relict glaucophane (GL-1, Tab. 1, Fig. 6) show slight depletion in chondrite-normalized light relative to heavy REEs ($[La/Lu]_N$ = 0.20-0.60); this chondrite-normalized REE pattern is similar to NMORB (REGELOUS et al. 1999), though most samples have lower absolute concentrations of REEs than NMORB. The other group of samples, including blueschist and greenschist facies samples (GL-2 and AECS, Tab. 1, Fig. 6), have strongly fractionated patterns of chondrite-normalized light to heavy REEs ($[La/Lu]_N$ = 1.09-3.08), with overall abundances greater than NMORB.

No.	14	15	16	17	18	19	20	21	22	23	24	25	26
SAMPLE	DR-1056/46	DR-113/6	DR-124/3	DR-124/10	DR-1058/1	DR-124/8	DR-124/9	DR-121/3	DR-113/2	905/1	909/1	n=12	n=10
ROCK	GL-1	GL-2	GL-2	GL-2	AECS	AECS	AECS	AECS	AECS	GRAMP	AMPH	GRAMP	AMPH
SiO_2	-	49.66	48.78	47.62	52.14	48.32	51.38	51.12	-	46.52	48.54	44.20	45.64
TiO_2	-	0.92	1.02	1.05	1.10	1.48	1.07	1.02	-	0.68	0.88	0.84	0.79
Al_2O_3	-	15.06	13.66	12.86	13.89	16.34	15.69	15.22	-	19.55	20.7	19.40	17.57
Fe_2O_3	-	3.52	4.46	3.23	4.97	4.62	3.30	2.67	-	3.96	3.4	4.26	3.99
FeO	-	5.52	5.39	5.84	8.97	6.98	5.26	5.68	-	5.01	5.17	7.04	6.09
MnO	-	0.16	0.15	0.31	0.36	0.24	0.20	0.13	-	0.14	0.16	0.20	0.13
MgO	-	9.02	10.07	8.73	6.60	6.95	6.91	9.98	-	5.61	4.21	6.35	8.52
CaO	-	6.59	7.80	10.76	4.85	5.04	6.31	4.07	-	13.12	9.96	12.15	12.81
Na_2O	-	4.83	3.78	4.21	4.49	5.44	4.86	4.71	-	2.22	3.26	2.16	1.80
K_2O	-	0.17	0.65	0.06	0.14	0.22	1.39	1.28	-	0.24	0.63	0.30	0.28
P_2O_5	-	0.26	0.24	0.32	0.20	0.41	0.32	0.26	-	0.05	0.14	0.09	0.04
LOI	-	4.40	4.00	5.00	2.30	4.09	3.34	3.87	-	2.43	2.91	2.70	2.29
TOTAL	-	100.11	100.00	99.99	100.00	100.04	100.00	100.00	-	99.53	99.96	99.67	99.96
La	0.28	7.48	5.12	8.31	1.74	15.90	11.00	10.50	17.70	2.75	4.05	-	-
Ce	0.93	16.40	12.60	20.70	6.32	41.70	28.50	25.80	35.10	6.5	9.75	-	-
Nd	0.87	10.60	9.10	12.90	6.42	24.50	18.90	16.70	29.40	4.32	5.8	-	-
Sm	0.46	3.80	2.50	3.51	2.65	6.40	4.20	4.60	5.60	1.25	1.54	-	-
Eu	0.24	0.98	0.90	1.16	1.15	2.11	1.48	1.48	1.67	0.46	0.98	-	-
Tb	0.176	0.61	0.65	0.63	0.82	1.25	0.68	1.02	0.86	0.2	0.31	-	-
Yb	0.657	2.245	2.04	2.22	3.50	3.80	2.31	3.09	2.54	0.37	0.9	-	-
Lu	0.10	0.28	0.28	0.27	0.52	0.54	0.32	0.39	0.29	0.056	0.15	-	-
TOTAL REE	3.713	42.395	33.19	49.70	23.12	96.20	67.39	63.58	93.16			-	-
Rb	0	0	0	0	0	0	0	29.2	45.7	-	-	-	-
Cs	-	-	-	-	-	-	-	-	-	-	-	-	-
Sr	663	0	0	0	0	0	0	0	0	-	-	-	-
Ba	-	-	-	-	-	-	-	-	-	-	-	-	-
Cr	16.6	96.7	102	117	56	46.7	70	30	70.5	-	-	-	-
Co	34.5	31.4	36.2	30	33.5	27.7	26	24.9	29.3	-	-	-	-
As	-	-	-	-	-	-	-	-	-	-	-	-	-
Sb	-	-	-	-	-	-	-	-	-	-	-	-	-
Sc	32.2	38.2	45.1	36	39.8	32.8	26	35.5	34.2	-	-	-	-
Hf	0	2.5	1.2	1.8	1.75	3.4	2.6	1.8	2.9	-	-	-	-
Th	0	1.5	0.95	1.1	0	1.6	1.4	1.5	2.3	-	-	-	-
U	-	-	-	-	-	-	-	-	-	-	-	-	-
Ta	0	0	0	0	0	0	0	0	2.5	-	-	-	-
Zr	-	-	-	-	-	-	-	-	-	-	-	-	-
Ni	-	-	-	-	-	-	-	-	-	-	-	-	-
Se	-	-	-	-	-	-	-	-	-	-	-	-	-
Zn	-	-	-	-	-	-	-	-	-	-	-	-	-

Isotopic data and ages

One metasomatized gabbro and one diorite from the Dzela metamorphic complex were collected for age determination. Th-U-Pb analyses of zircons from these samples were performed using a Cameca IMS1270 ion-microprobe at the NORDSIM Facility, Swedish Museum of Natural History, Stockholm, by V. Pease (REMIZOV & PEASE 2004). Analytical procedures are similar to those described by WHITEHOUSE et al. (1997, 1999). Common Pb corrections were made using the measured ^{204}Pb signal assuming a STACEY & KRAMERS (1975) composition of the appropriate age. The ion beam was typically oval with a longer dimension of c. 25 µm. The data are plotted on inverse concordia (Tera-Wasserburg) diagrams ($^{207}Pb/^{206}Pb$ vs. $^{238}U/^{206}Pb$). Concordia ages are reported at the 2σ confidence level (LUDWIG 1998) and are indicated by shaded ellipses. Analyses >5 % discordant were not included in the final age determinations.

Sample VP97-029, metadiorite

The sample came from a highly-sheared leucocratic interlayer within amphibolite, which is regionally associated with pyroxenite. The leucocratic layer has a layer-parallel foliation striking NE 55 °E and dipping vertically. It is concordant with the foliation of the amphibolite. Petrographically, it is composed of zoisite poikiloblastically enclosing plagioclase relics and randomly oriented muscovite, all within a groundmass of plagioclase. Minor alteration of groundmass plagioclase to sericite occurs along plagioclase cleavage planes. Only nine zircon grains of variable morphology were separated from c. 4 kg of sample. All nine grains were analyzed and gave generally concordant results (7 out of 9 grains). Two populations are defined (Fig. 7a). The oscillatory zoned cores represent an older population which yields a concordia age of 501 ±9.7 Ma. The bright amorphous rims and the leached grains define a younger population with a concordia age of 350 ±11 Ma.

We interpret the older age to represent the time of migmatite genesis, i.e. crystallization during a high-grade (amphibolite facies) metamorphic event. The younger age is correlated with a major high-pressure metamorphic event. This event at c. 360 Ma is well defined along the length of the Urals west of the MUF; it is thought to represent the closure of the Uralian paleo-ocean.

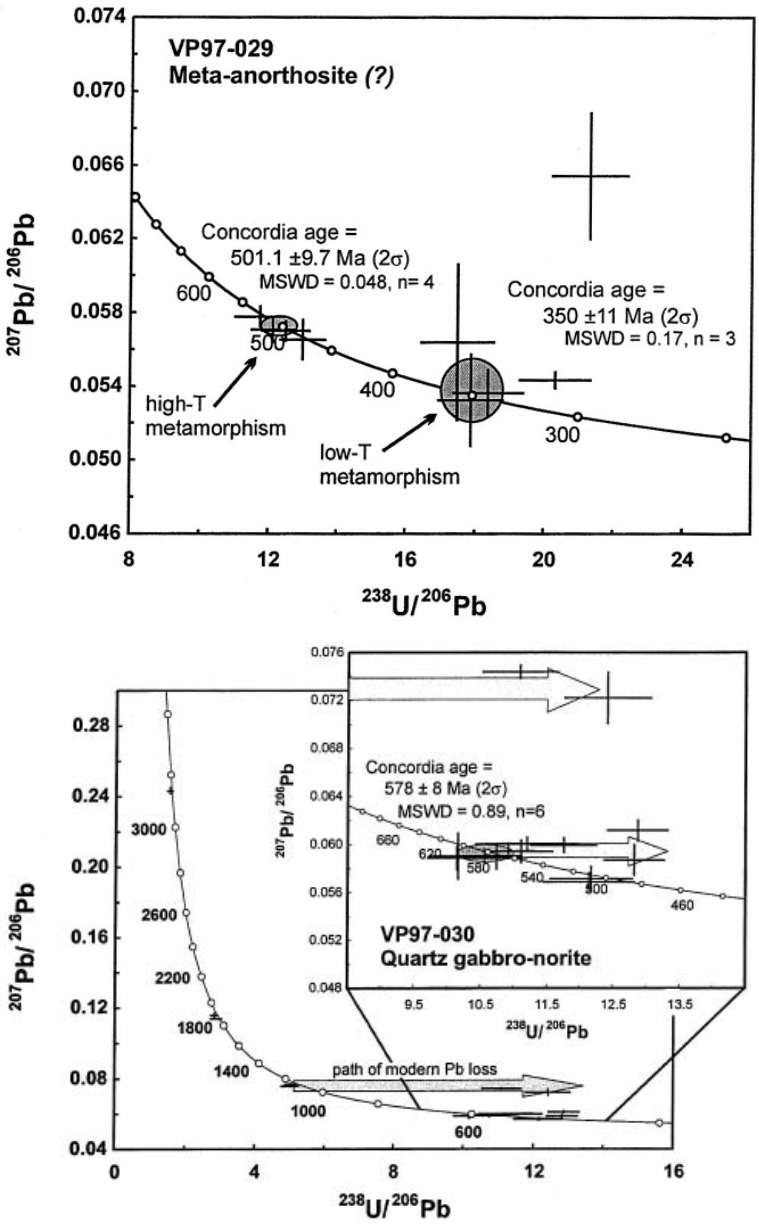

Fig. 7: Inverse concordia diagrams for samples from the Dzela metamorphic complex (from REMIZOV & PEASE 2004). For sample locations see Fig. 5.
a) Inverse concordia diagram for the foliated meta-diorite sample VP97-029. All analytical data are plotted with 1 σ error bars, while concordia ages (LUDWIG 1998) are reported at the 2 σ confidence level and are indicated by shaded ellipses (analyses >5 % discordant were not included in the final analysis). Two metamorphic age populations are defined.
b) Inverse concordia diagram for the quartz gabbronorite sample VP97-030. All analytical data are plotted with 1 σ error bars, while concordia ages (LUDWIG 1998) are reported at the 2 σ confidence level and are indicated by shaded ellipses (analyses >5 discordant were not included in the final analysis). The protolith crystallization age is defined.

Abb. 7: Konkordia-Diagramme für Proben vom metamorphen Dzela-Komplex (aus REMIZOV & PEASE 2004). Lage der Probenpunkte siehe Abb. 5.

Sample VP97-030, quartz gabbronorite

The sample came from a low-strain domain of regional amphibolite facies metamorphism. Intrusive relationships are preserved between members of a mafic igneous complex. The foliation, when present, strikes E-W and dips variably. Younger cross-cutting fractures, faults, and andesite (?) dykes trend NE-SW, parallel to the MUF. Petrographically, the sample comprises a diorite in amphibolite facies. A good zircon yield was obtained from c. 3 kg of sample material. Nineteen grains were analyzed with complex results (Fig. 7b). There is a large proportion (26 %) of concordant older dates between 1.09 and 3.14 Ga. There is also a significant proportion (32 %) of concordant dates that give a concordia age of 578 ±8 Ma. In addition, there appear to be concordant dates at c. 500 Ma and many (32 %) significantly discordant analyses. All of these analyses, however, are associated with either high-U and/or Th zircons, grain fractures, or leached grains.

These data, along with published information on the geological structure of the Polar Urals, allow us to make inferences regarding the processes of island-arc formation which were involved in the generation of the Dzela Complex. The oceanic crust of the Dzela Complex was formed 578 ±8 Ma ago.

CONCLUSIONS

These and other data published in REMIZOV (2004) allow the probable mechanism of the beginning of the formation of the intra-oceanic island arc to be inferred. The main mechanism described is folding of oceanic crust in the initial stages of subduction. At first, the subduction rate was slow and oceanic crust had to deform via folding. After the main folding, which formed the foreland, the lower part of the fold warmed up and became plastic. This enabled upper part of the oceanic crust to be forced into the basement of the future island arc. The temperature increased to around that of the onset of melting. A mixture of oceanic basalt, oceanic sediment, gabbro and formerly depleted mantle was melted and this association generated boninitic magma at a depth of 30-45 km. It is probable that the ultramafic rocks of the Dzela Complex were

partially melted at the beginning of island-arc formation. This is indicated by the "boninitic" signature in their REE pattern and Eu anomaly (garnet pyroxenites and plagioclase lherzolites). Al+Ca+Si±Na metasomatism took place during the main metamorphic event; this was followed by fluid enrichment from the subduction zone. The overlying rocks were eclogitized "above the accretion zone" and fixed there. The Dzela and Khord"yus rocks belong to the upper parts of similar complexes. Amphibolite-facies metamorphism of the Dzela Complex occurred at 501 ±10 Ma.

Exhumation of the Dzela Complex took place during collision between the passive margin of the East European craton (Baltica) and the Voikar island arc. In time, the amphibolite-facies Dzela Complex was metamorphosed under blueschist-facies conditions. The complex includes a portion of the oceanic crust which was subducted and then brought to increasingly higher crustal levels. This oceanic crust includes oceanic basalt and basaltic tuff with rare layers of metasedimentary jasper. The significance of this work is the identification of remnants of Precambrian oceanic crust entrained within the structure of the Polar Urals and the evidence that the paleo-Ural ocean existed continuously from Precambrian time until c. 360 Ma ago.

ACKNOWLEDGMENTS

The author is greatly indebted to Vicky Pease for the geochronological Zr data, and to the Swedish National Science Research Council, Uppsala University, the Swedish Museum of Natural History, and EU INTAS grant no. 97-1139 for invaluable support.

The paper was compiled during the author's stay at the Federal Institute for Geosciences and Natural Resources in Hannover funded by the German Ministry of Education and Research (BMBF) within the scope of the Russian-German co-operation in science and technology (WTZ). The author gratefully acknowledges this financial support. He thanks Hans Paech (Potsdam) who translated large parts of the paper into English and Henry Toms for improving the English text. Solveig Estrada is thanked for her support during preparation of the manuscript, and particularly Klaus Burgath for his very valuable remarks.

References

Becker, H., Jochum, K. & Carlson, R. (2000): Trace element fractionation during dehydration of eclogites from high-pressure terranes and the implications for element fluxes in subduction zones.- Chem. Geol. 163:65-99.

Boynton, W. (1984): Geochemistry of the rare earth element: Meteorite studies.- In: R. HENDERSON (ed). Rare Earth Element Geochemistry. Elsevier, Amsterdam, 63-114.

Dobretsov, N.L. (1974): Glaucophane schist and eclogite-glaucophane schist complexes in the USSR.- Nauka, Novosibirsk, 1- 436 (in Russian).

Efimov, A.A. & Potapova T.A. (1990): The tectonics of the bottom (metabasic) structural unit of the Voikar Ophiolitic allochthon in the Polar Urals.- Geotektonika 5:45-54 (in Russian).

Efimov, A.A. & Potapova, T.A. (2000): High-pressure metagabbroic complexes in ophiolites of the Polar Urals: "Counter-clockwise" metamorphism related to a Paleozoic subduction zone.- In: Magmatic and metamorphic formations of Ural and their metallogeny. Ekaterinburg, 233-268 (in Russian).

Fershtater, G.B. (1987): Petrology of the main intrusive associations.- Nauka, Moscow, 1-232 (in Russian).

Kostyukhin, M.N. & Remizov, D.N (1995): Petrology of ophiolites from the Khadatin gabbro-ultramafic massif (Polar Urals).- Nauka, St. Petersburg, 1-120 (in Russian).

Ludwig, K. (1998): On the treatment of concordant uranium-lead ages.- Geochim. Cosmochim. Acta 62:665-676.

Mocek, B. (2001): Geochemical evidence for arc-type volcanism in the Aegean Sea: the blueschist unit of Siphnos, Cyclades (Greece).- Lithos 57:262-289.

Perfil'ev, A.S. (1979): The Uralian geosyncline and the development of the Earth's crust.- Nauka, Moscow, 1-188 (in Russian).

Polat, A., Hofmann, A., Munker, C., Regelous, M. & Apple, P. (2003): Contrasting geochemical patterns in the 3.7-3.8 Ga pillow basalt cores and rims, Isua Greenstone Belt, southwest Greenland: Implications for postmagmatic alteration processes.- Geochim. Cosmochim. Acta 67:441-457.

Puchkov, V.N. (1979): Bathyal complexes of geosyncline passive margins.- Nauka, Moscow, 1-260 (in Russian).

Pystin, A.M. (1994): Polymetamorphic complexes of the western slope of Urals.- Nauka, St. Petersburg, 1-209 (in Russian).

Regelous, M., Niu, Y., Wendi, J., Batiza, R., Greig, A. & Collerson, K. (1999): Variations in the geochemistry of magmatism on the East Pacific Rise at 10°30'N since 800 ka.- Earth Planet. Sci. Letters 168:45-63.

Remizov, D.N. (2000): The evolution of the island arc system of the Polar Urals.- II. Petrologic Congress of Russia, Syktyvkar, 135-138 (in Russian).

Remizov, D.N. (2004): The Paleozoic island arc system of the Polar Urals.- Ekaterinburg, 1-222 (in Russian).

Remizov, D.N. & Pease, V. (2004): The Dzela Complex, Polar Urals, Russia: a Neoproterozoic island arc.- In: D. GEE & V. PEASE (eds). The Neoproterozoic Timanide Orogen of eastern Baltica, Mem. Geol. Soc. London 30:107-123.

Savel'eva, G.N. (1987): Gabbro-ultrabasite assemblages of Uralian ophiolites and their analogues in recent oceanic crust.- Nauka, Moscow, 1-242 (in Russian).

Stacey, J. & Kramers, J. (1975): Approximation of terrestrial lead isotope evolution by a two-stage model.- Earth Planet. Sci. Letters 26:207-221.

Valizer, P.M. & Lennykh, V.I. (1988): Amphiboles of Uralian blueschists.- Nauka, Moscow, 1-203 (in Russian).

Yazeva, R.G. & Bochkarev, V.V. (1984): Voikar volcano-plutonic complex (Polar Urals).- Ural. Sc. Centre USSR, Sverdlovsk, 1-160 (in Russian).

Yudin, V.V. (1994): Orogeny of northern Urals and Pai-Khoi.- Nauka, Ekaterinburg, 1-286 (in Russian).

Whitehouse, M., Claesson, S., Sunde, T. & Vestin, J. (1997): Ion-microprobe U-Pb zircon geochronology and correlation of Archaean gneisses from the Lewisian Complex of Gruinard Bay, northwestern Scotland.- Geochim. Cosmochim. Acta 61:4429-4438.

Whitehouse, M.J., Kamber, B. & Moorbath, S. (1999): Age significance of U-Th-Pb zircon data from early Archaean rocks of west Greenland – a reassessment based on combined ion-microprobe and imaging studies.- Chem. Geol. 160: 201-224.